



Research Article

Zoology

Ultrastructural Investigation of the Brain Neuroanatomy in Adult *Rhinopoma hardwickii*

Eman E. El-Nahass, Atteyat Selim, Omnia Shahin*

Zoology Department, Faculty of Science, Tanta University, Tanta 31527, Egypt.

Received: 8/5/2025

Accepted: 31/5/2025

KEY WORDS

Astrocytes, Bats,
Brain,
Cerebellum,
Microglia,
Neurons,
Oligodendrocyte,
Pyramidal
neurons

ABSTRACT

Microchiropteran *Rhinopoma hardwickii* can echolocate during self-powered flight, unlike other Megachiropterans. This study aimed to examine the ultrastructural characteristics of various adult *R. hardwickii* brain regions. Two adult bats were euthanized via cervical dislocation, and their brains were preserved in glutaraldehyde, followed by rinsing in cacodylate buffer, and then post-fixed with osmium tetroxide. Samples were dehydrated using ethyl alcohol, and then embedded in epoxy resin. For tissue examination, semi-thin sections were stained with toluidine blue, and then the ultrathin sections were stained with uranyl acetate dihydrate and a saturated lead citrate solution. The sections were examined and photographed. The brain is divided into three regions: the forebrain, midbrain (hippocampus), and hindbrain. Using a transmission electron microscope, the brain comprises blood vessels and two cell types: neurons and their supporting glial cells. Neurons appeared as large cells with neuronal processes, they have large nuclei with diffuse chromatin and prominent nucleolus. It has two types: large flask pyramidal cells with a single robust, cortically aligned apical dendrite and several basal dendrites and small non-pyramidal cells that may be stellate or granule cells. Glial cells were well developed, especially in the cerebellum, having four types: astrocytes, microglia, oligodendrocytes, and ependymal cells. This study concluded that the brain of *R. hardwickii* characterized by its diminutive size and increased number of well-developed neurons, particularly in the cerebellum relative to other brain parts; it also discloses neurological traits linked to echolocation, revealing evolutionary affinities and relationships of chiropteran.

Introduction

The brain is a highly complex organ with many regions that vary in cellular structure and connection patterns (Turegano-Lopez et al., 2024). A major challenge in neuroscience is deciphering the brain's structural layout (DeFelipe, 2010). The neuroanatomical structure is fundamental for comprehending brain functions and disorders (Li et al., 2010). Despite advancements in light microscopy, only electron microscopy (EM) can elucidate every axon, dendrite, and synaptic connection inside a neuropil volume (Knott et al., 2008). For several decades, transmission electron microscopy (TEM) has been employed to examine neuronal ultrastructure, commencing with the initial categorization of synapses in the cerebral cortex (Grey, 1959) and progressing to detailed serial section analyses of substantial segments of identified neurons (White and Rock, 1980; Anderson et al., 1994). The application of electron-dense staining through immunohistochemical electron microscopy has enabled the identification of microglial cell bodies and processes, which were difficult to discern using traditional electron microscopy. It has illuminated their complex interactions with neurons and synapses (Tremblay et al., 2010).

Over the past six decades, ultrastructural analyses have provided substantial insights into the functional roles of neurons, synapses, and glial cells across various conditions (Theodosis et al., 2008; Paolicelli et al., 2011; Bourne and Harris, 2012; Schafer et al., 2012; Kettenmann et al., 2013; Knott and Genoud, 2013; Chung et al., 2015; Verkhatsky and Nedergaard, 2018).

The neuronal, microglial, astrocytic, and oligodendrocytic compartments can be distinguished by electron microscopy according to their distinct morphology, dimensions, nuclear heterochromatin patterns, organelles, cytoskeletal components, and interrelationships within the brain parenchyma. Plasma membranes, basement membranes, clefts in gap junctions, actin filaments, intermediate filaments, microtubules, ribosomes, extracellular spaces, glycogen granules, synaptic vesicles, dense-core vesicles, nuclear pores, and lysosomes are exclusively or optimally visualized using electron microscopy (EM), achieving the highest resolution of up to 1 nm for a biological technique. Significant functions of microglia have been discovered, particularly because of the ultrastructural resolution exclusively achievable through electron microscopy (Savage et al., 2018).

In both young adult and aged mice, astrocytes exhibited a relative paucity of electron-dense material inside the cytoplasm. Moreover, astrocytic cell bodies and processes displayed mitochondrial membranes that were less electron-dense than those found in neighboring neuronal and glial structures, including neurons, dendrites, microglia, oligodendrocytes, as well as in the endothelium and pericytes (Nahirney et al., 2016). Examining the synaptic foundation of neural networks within a brain tissue volume necessitates electron microscopy, featuring a resolution sufficient to observe the minutest synaptic connections (Knott et al., 2008).

While there is limited research on the ultrastructure of bat brain cells with EM,

several studies provide valuable insights into related areas. For instance, **Feng and Popper (1998)** observed significant heterogeneity in brain anatomy among bat species influenced by ecological and behavioral factors. Nectarivorous bats, such as *Glossophaga soricina*, possess a comparatively larger visual cortex than insectivorous bats, indicating their need for visual signals for navigation and food source recognition. In contrast, species reliant on echolocation, like *Myotis brandtii* and *Pipistrellus pipistrellus*, demonstrate highly specialized auditory processing areas in the brain, characterized by enhanced synaptic organization in the auditory cortex (**Kowalski et al., 1996**).

(**Kang et al., 1985**) examined the posterior hypothalamus of hibernating greater horseshoe bats (*Rhinolophus ferrumequinum*) and identified three types of neurons: the first type was the largest, exhibiting an oval or conical morphology, with an elliptical nucleus and a nuclear envelope characterized by numerous deep invaginations. The cell organelles were highly developed, notably with plenty of variably shaped mitochondria, alongside the Golgi complex and polysomes in the cytoplasm. The second form of the neuron was of intermediate size, ovoid or elliptical, with the nucleus positioned closer to the plasma membrane and the nuclear envelope exhibiting minimal invaginations. The cytoplasm was abundant and the cell organelles, particularly the rough endoplasmic reticulum, were highly developed. Lipofuscin pigments were also found. The third type was the smallest in dimension and spherical in form. The nucleus and nucleolus were seen in the middle region of the cell body, and the

nuclear envelope exhibited several invaginations. The cytoplasm was diminutive compared to the first and second types, yet the rough endoplasmic reticulum, mitochondria, and polysomes were comparatively well-developed. The cytoplasm exhibited membrane-bound organelles with a single membrane containing a delicate particulate material surrounding the rough endoplasmic reticulum and Golgi complexes. Due to the scarcity of EM studies on bats' brain, this study aimed to investigate the neuroanatomy of the brain in adult *R. hardwickii*.

Material and Methods

Bats Sampling Collection

The current study utilized adult, normally healthy bats of the *R. hardwickii* species taken alive from Egyptian caves in Abu Rawash. These bats had to be free of any anatomical abnormalities. After using an Anahal (isoflurane) solution, the bats were anesthetized, sacrificed, and allowed to bleed and gather brain samples.

Stereoscopic microscopic examination

The skin and muscles were removed from the skull and neck; the head was detached at the neck and submerged in fixative for several hours, after which the calvarium and the dorsal portion of the upper cervical vertebrae were excised. The exposed brain was thereafter immersed in the fixative for many additional hours, after which the morphological characteristics of the brain were described. The photomicrographs of the brain were taken using the Stereo Microscope Stemi 508 and a Canon Power Shot A95 camera linked to a Carl Zeiss Microscopy GmbH. According to the Nomina Anatomica Mammalia (**Baumel**

et al., 1993), the anatomical terms were written.

Transmission electron microscopic examination

For The preparation of semi-thin sections, two adult studied bats were used for the Transmission electron microscopic investigations. Following the dissection of bat cranium, the brain specimens were removed carefully from position, sliced into small portions of 1-MM3 sections and processed quickly according to the protocol of TEM with the following steps: Fixation in 2.5% glutaraldehyde for 24 hours, followed by rinsing in 0.1 M cacodylate buffer at pH 7.4, and then post-fixation for 1 hour at room temperature with 1% osmium tetroxide. Samples were dehydrated using ethyl alcohol in a sequential gradient and subsequently embedded in epoxy resin (Kandyel et al., 2021). For tissue analysis, semi-thin slices (0.5 µm thickness) were prepared and stained with toluidine blue (Spurr, 1969), subsequently examined and photographed using a light microscope (Leitz Dialux 20, Leica DMLS) in conjunction with a digital camera (Canon PowerShot A95).

Ultrathin slices (50–60 µm) were prepared and stained using uranyl acetate dihydrate and a saturated lead citrate solution (Bozzola and Russell., 1992). The slices were ultimately imaged using a JEOL JEM-2100 TEM at the Faculty of Agriculture, Mansoura University, Egypt. The TEM photographs were processed, enlarged, printed, and investigated.

Ethical statements

This study was prepared according to the guidelines provided by Tanta University, Faculty of Science's Committee on Animal Welfare and Ethics, and

Egyptian laws, with the reference number (IACUC-SCI-TU-0342).

Result

Examination of gross morphological brain structures

R. hardwickii is a diminutive bat characterized by a reduced brain in size that was entirely located in the cranium. After removing the meninges covering, the brain appeared ovoid with thin, pointed rostral end and gradually widened caudal end of the cerebral hemisphere. The dorsal surface of cerebrum was mainly lissencephalic devoid of usual gyri and sulci. The brain was organized into the forebrain, midbrain containing the hippocampus and it was the most rostral part of the brainstem (pons and medulla oblongata), and hindbrain containing the cerebellum (Fig. 1a).

Transmission electron microscopic observations

The brain comprised blood vessels and two main cell types: neurons and their supporting glial cells.

Neurons: Large cells with basophilic cytoplasm, large nucleus with diffuse chromatin, and prominent nucleolus and neuronal process. It had two types: large pyramidal and small non-pyramidal cells (stellate or granular). In these neurons, especially those involved in neurotransmitter production or processing, a well-developed prominent rough endoplasmic reticulum (RER) was present for protein synthesis, particularly in the cell body. Also, the Golgi apparatus can be seen near the nucleus, processing and packaging proteins for secretion or membrane insertion.

Glial cells have four types: Astrocytes, microglia, oligodendrocytes, and ependymal cells.

Transmission electron microscopic observations of the forebrain

The cerebral cortex was made up of neurons with diverse morphologies. It may be pyramidal and non-pyramidal neurons, including their dendritic spines, synaptic vesicles, and axonal terminals. These neurons had organelles, including mitochondria, endoplasmic reticulum, and Golgi apparatus.

Pyramidal cells were larger in size, 10 to 80 micrometers in diameter, and resembled a flask with a single thick, cortically aligned apical dendrite alongside several basal dendrites. A significant type of pyramidal cell was the Betz cell, which lied within the primary motor cortex (**Figs. 1b, c**).

Non-pyramidal stellate cells: smaller in size, 5 to 15 micrometers in diameter, it had organelles including mitochondria that may be hypertrophied, endoplasmic reticulum, and Golgi apparatus (**Fig. 1d**).

Axon terminals made synaptic connections between neurons in the forebrain appeared with the synaptic cleft, synaptic vesicles, dendritic spines, or other axons. In the presynaptic terminals, **neurotransmitter synaptic vesicles** were observed containing neurotransmitters. Depending on the neurotransmitter being stored, these vesicles can be either clear or dense (**Figs. 2a-d**).

The forebrain's white matter contained myelinated axons, the myelin sheaths produced by oligodendrocytes. These sheaths provided insulation to the axons and were essential for fast signal transmission. Axons were integrated, forming axonal projection pathways through which brain regions communicate with other parts, such as the thalamus and cortex. The myelin sheath had gaps named **Nodes of**

Ranvier in which the voltage-gated ion channels were clustered, facilitating salutatory conduction and the rapid transmission of action potentials (**Figs. 2e, f**).

Transmission electron microscopic observations of the midbrain (hippocampus)

The midbrain was located between the forebrain and hindbrain and was involved in functions like motor control, vision, and hearing.

Neurons have two types;

Granular non-pyramidal neurons had granulated cytoplasm and a large nucleus with heterochromatin scattered in the nucleoplasm (**Figs. 3a, b**).

Pyramidal neurons appeared with large cell bodies, a centrally located nucleus, and numerous mitochondria present in the cytoplasm. They also had dendrites with spiny projections for synaptic contact (**Fig. 3c**).

Glial cells (fibrous astrocytes that appeared in long, thin, unbranched processes) supported neurons and can be identified by their extensive, star-shaped processes (**Fig. 3d**).

Transmission electron microscopic observations of the hindbrain

The hindbrain consisted of cerebellum. It revealed detailed features of the cellular components and their organization, highlighting the intricate organization of neurons, synapses, and glial cells that supported their functions in motor control, autonomic regulation, and coordination.

The electron microscopy of the cerebellum

Neurons:

Large, unique neurons were found in the cerebellar cortex, which contained large, elliptic nuclei with nuclear envelopes had deep invaginations with prominent

nucleoli. These neurons had well-developed vacuolated cytoplasm comprising many organelles, including mitochondria, rough endoplasmic reticulum (RER), and Golgi apparatus (**Figs. 4a, b**).

Cerebellum Specific Features

Purkinje cells had an extensive dendritic tree densely covered with spiny dendrites. The dendrites were in close contact with the parallel fibers from granule cells, forming synapses (**Fig. 4c**). The dendritic spines (small protrusions) can be seen near presynaptic terminals. These purkinje cell dendrites and axonal fibers from granule cells were found in the molecular outermost layer of the cerebellum.

Glial cells:

Star-shaped protoplasmic astrocytes had thick and branched processes that enveloped blood vessels and synapses. They were attached to neurons and vessels, provided structural support to neurons, guide neuronal migration and brain plasticity, determined capillary permeability, interact with neurons and blood vessels (Blood-brain barrier), and helped in neurotransmitter uptake (**Figs. 5a, b**).

Vasculature: Blood vessels in the hindbrain showed the endothelial cells forming the blood-brain barrier. Pericytes and astrocyte processes surrounded the blood vessels, providing structural support and regulating the blood-brain barrier (**Fig. 5c**).

Blood-Brain Barrier: This barrier was formed by the endothelial cells that lined the blood vessels and were tightly joined. These endothelial cells and tight junctions help in protecting the brain from harmful substances while allowing nutrients to pass through (**Figs. 5b, c**).

Ciliated ependymal cells appeared cuboidal-shaped. They lined the brain's ventricles and produced cerebrospinal fluid (CSF). Cilia on these cells tracked into the CSF and helped circulate it. They formed a permeable barrier between the CSF-filled cavities and the brain tissue (**Figs. 5d, e**).

Small microglia cells (the brain's resident immune cells) with a darkly staining nucleus and thorny processes extending toward areas of injury or inflammation, which help monitor neuronal health, can morph into a special type of macrophage that can phagocytose pathogens or dead neurons (**Fig. 5f**).

Transmission electron microscopic observations of the midline structures (brain stem; medulla oblongata and pons)

The medulla oblongata:

Contained nuclei for autonomic functions with dense neuronal networks and synaptic contacts. It regulated vital autonomic functions such as heart rate and respiration. Well-organized neuronal clusters and dense synaptic networks, particularly in regions such as the nucleus of the solitary tract and the dorsal motor nucleus of the vagus nerve (**Fig. 6a**).

The pons:

Involved in motor coordination and had well-defined synaptic structures for communication between the brainstem and cerebellum. It contained motor neurons, relay neurons, and reticular formation neurons. The axons of these neurons travelled to the cerebellum and spinal cord. The synaptic organization in the pons was intricate, facilitating communication between the cerebellum and the brainstem (**Fig. 6b**).

Glial cells: Oligodendrocytes with small, condensed, round nuclei and clear cytoplasm appeared as the so-called "fried egg appearance". It's found in areas of the hindbrain where myelinated axons are abundant (e.g., in the pons or medulla); it was responsible for the myelination of axons visible as cells with multiple processes wrapping around axonal segments (**Fig. 6b**).

Axons were involved in the transmission of action potentials over long distances. They can be myelinated or unmyelinated; myelinated axons had a layered appearance due to the myelin sheath (**Figs. 6a, b**).

Synapses presynaptic terminals: were densely packed with synaptic vesicles containing neurotransmitters, which may be clear or dense, depending on the type of neurotransmitter (**Fig. 6a**).

Neurotransmitter vesicles: the hindbrain's presynaptic terminals contain synaptic vesicles filled with neurotransmitters such as glutamate, GABA, and acetylcholine. These vesicles help in synaptic transmission between neurons (**Fig. 6b**).

Postsynaptic densities: were areas of the dendritic membrane where synaptic receptors were located, often appearing as electron-dense regions (**Figs. 6a, b**).

Axodendritic synapses were synapses between axons and dendrites, prominent in regions like the pons and cerebellum (**Fig. 6a**).

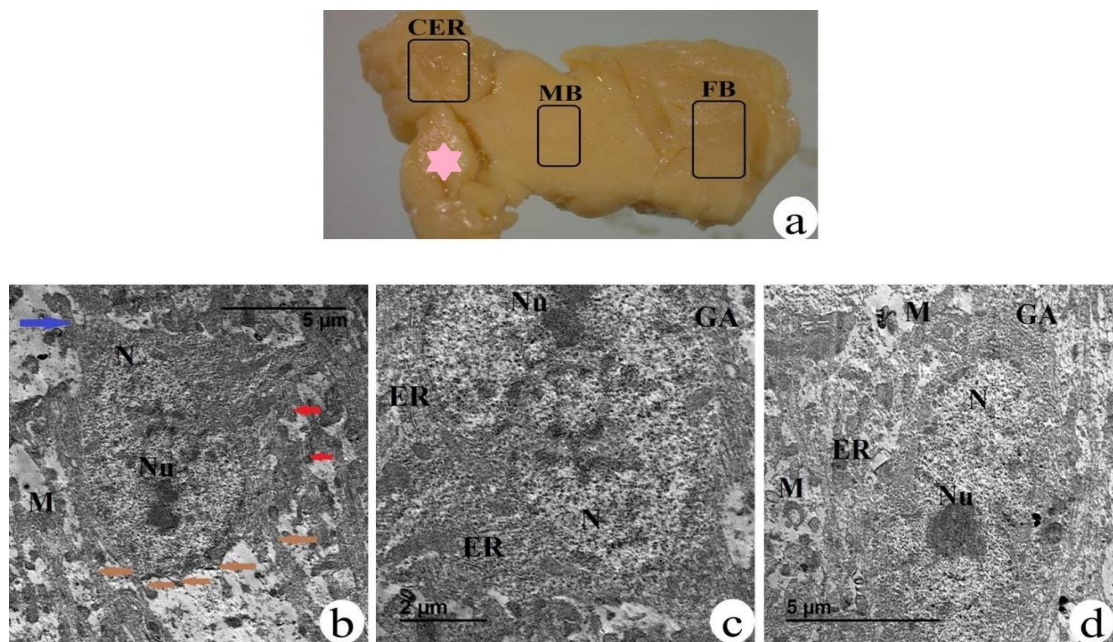


Fig. (1): **a**) Photomicrograph of a longitudinal section of the brain of adult Egyptian insectivorous Bat *Rhinopoma hardwickii* with a stereo microscope showing different brain parts: forebrain (FB), middle brain (MB), cerebellum (CER) in the hindbrain, and midline structures (pink star). **b-d**) Transmission electron micrographs of the cerebral cortex of *R. hardwickii* showing: **b,c**) Low and high magnification of large flask shaped pyramidal neurons, including their apical dendrite (blue arrow) and multiple basal dendrites with dendritic spines (brown arrows), synaptic vesicles (red arrows), and axonal terminals. These neurons have mitochondria (M), endoplasmic reticulum (ER), and Golgi apparatus (GA). **d**) Small stellate non-pyramidal neurons with mitochondria (M) that may be hypertrophied, endoplasmic reticulum (ER), and Golgi apparatus (GA).

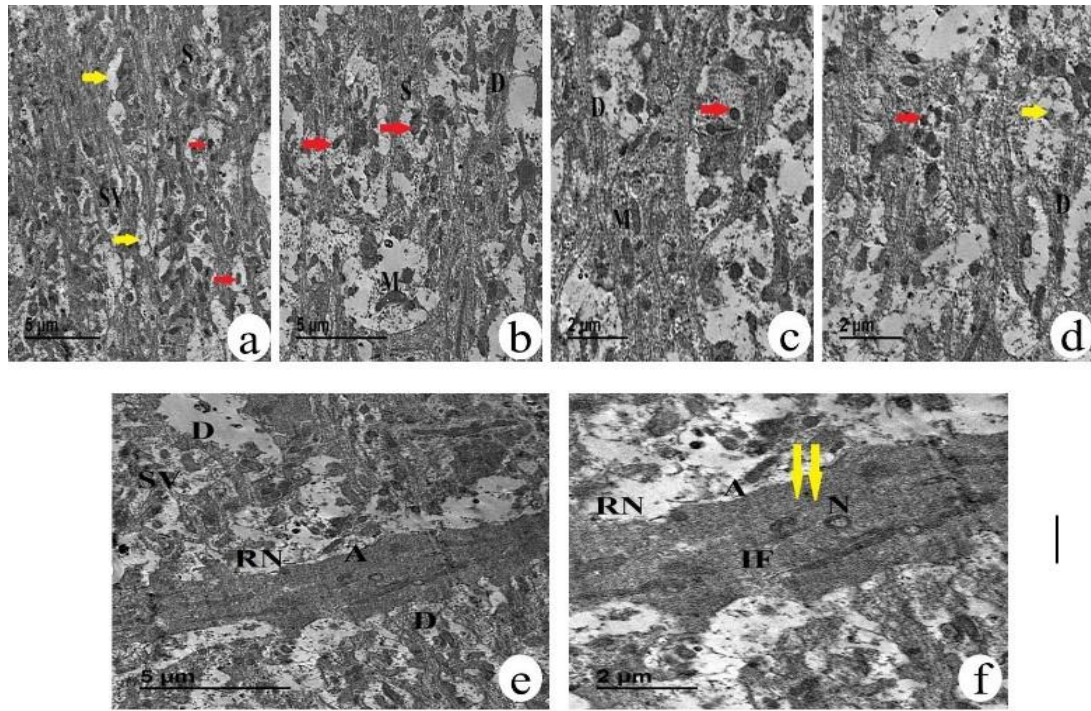


Fig. (2): a-d) Transmission electron micrographs of the forebrain's gray matter of *R. hardwickii* containing the synaptic connections between neurons appeared with the synaptic cleft (S), synaptic vesicles (SV), and the postsynaptic density had neurotransmitter receptors. Depending on the neurotransmitter being stored, these vesicles can be either clear (yellow arrow) or dense (red arrow). e, f) Transmission electron micrographs of low and high magnification of the forebrain's white matter of *R. hardwickii* containing myelinated axons (A) appear with a layered appearance due to myelin sheaths (double yellow arrows); this myelin sheath had gaps named Nodes of Ranvier (RN). Axon terminals make synaptic contacts (vesicles) with dendritic spines (D) or other axons.

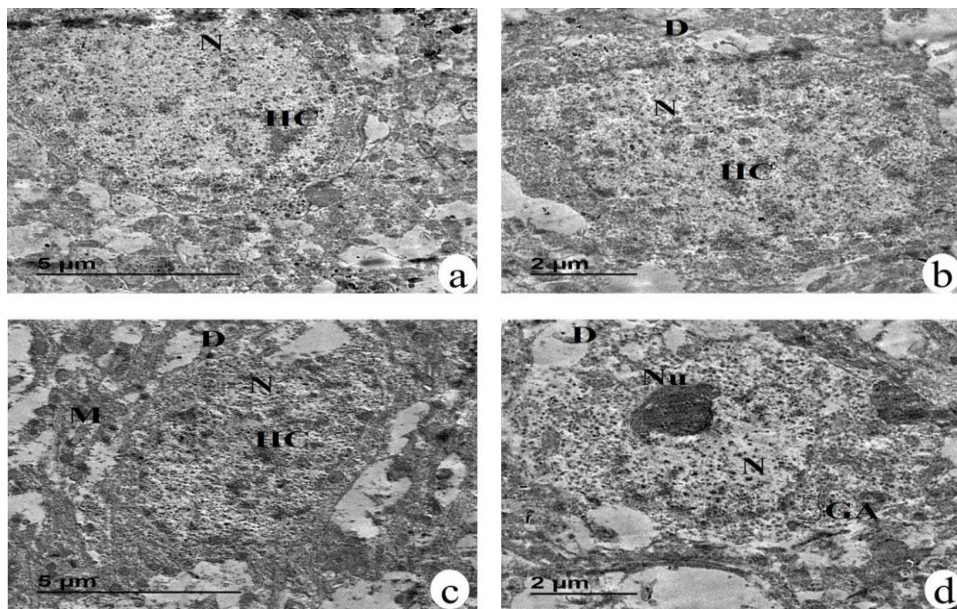


Fig. (3): Transmission electron micrographs of the midbrain (hippocampus) of *R. hardwickii* showing a, b) Low and high magnification of granular non-pyramidal neurons with dendrites (D), granulated cytoplasm, and large nucleus (N) containing heterochromatin (HC) scattered in the nucleoplasm. c) Pyramidal neurons appeared with large cell bodies; dendrites with spiny projections for synaptic contact (D), centrally located nucleus (N) with heterochromatin (HC), and numerous mitochondria (M) are present in the cytoplasm. d) Glial cells (astrocytes) support neurons can be identified by their extensive, star-shaped processes, dendrites (D), nucleus (N) with well-developed nucleolus (Nu) and Golgi apparatus (GA).

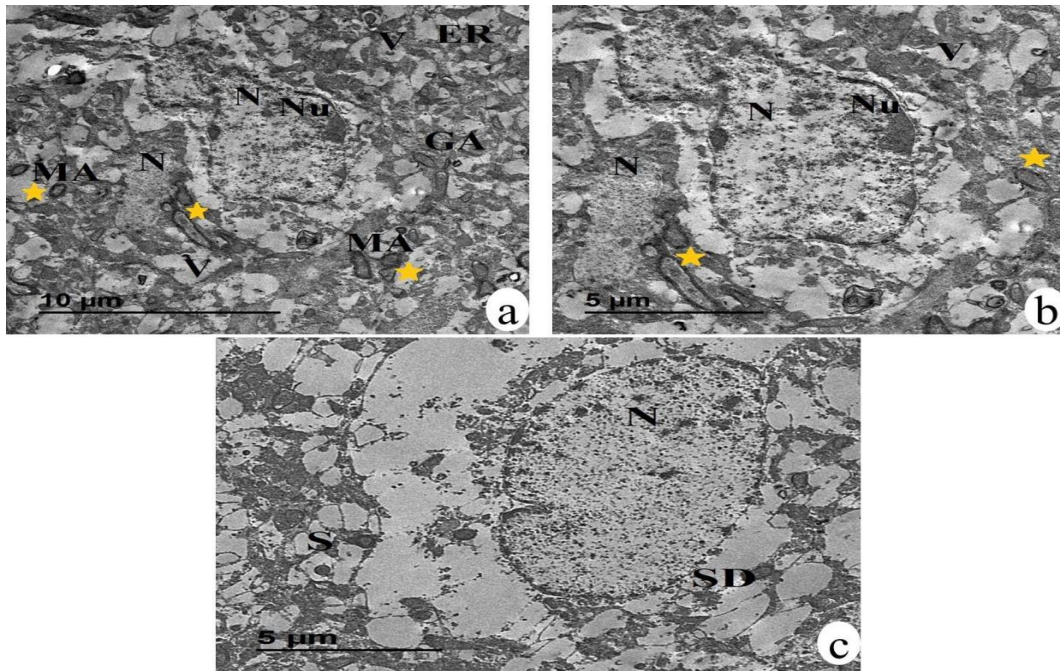


Fig. (4): Transmission electron micrographs of the hindbrain (cerebellum) of *R. hardwickii* showing **a, b**) Low and high magnification of the neurons with large cell bodies, irregular nuclei (N) with prominent nucleoli (Nu), well-developed cytoplasm with numerous organelles including mitochondria (M), endoplasmic reticulum (ER), and Golgi apparatus (GA). **c**) Purkinje cells have a large nucleus (N), an extensive dendritic tree that is densely covered with spiny dendrites (SD). The dendrites are in close contact with the parallel fibers from granule cells, forming synapses (S).

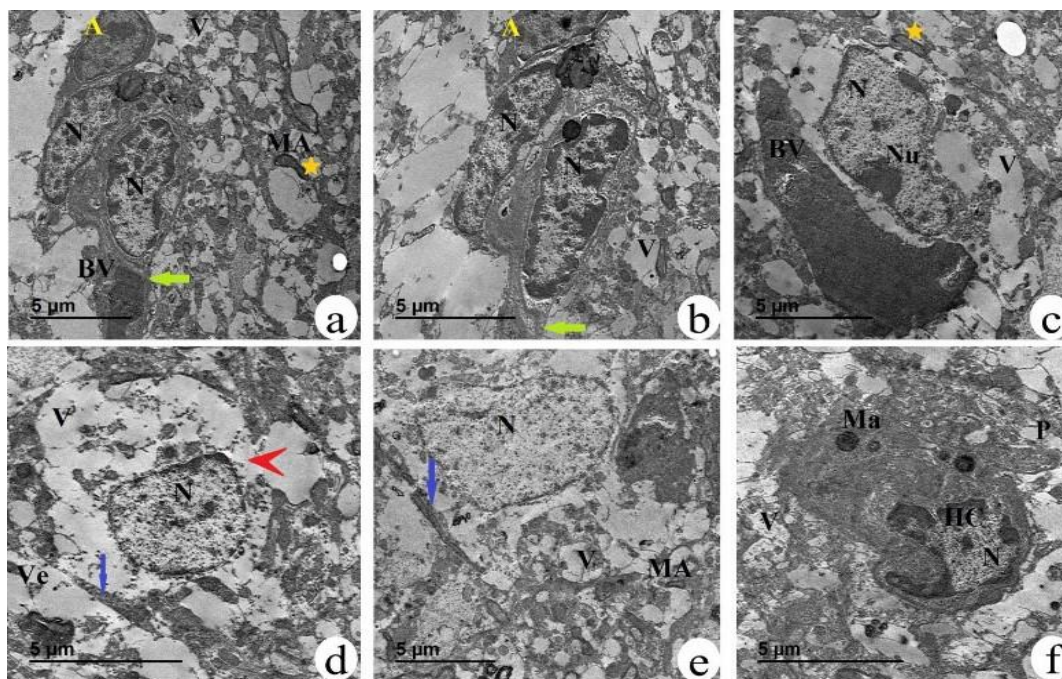


Fig. (5): Transmission electron micrographs of the hindbrain (cerebellum) of *R. hardwickii* showing **a, b**) Low and high magnification of star-shaped astrocytes (A) interact with neurons (N) and blood vessels making (Blood-Brain-Barrier) (green arrow), their processes can be seen enveloping blood vessels (BV) and synapses, the cytoplasm has vacuoles (V) and myelinated axons (MA, orange star). **c**) Blood vessels in the hindbrain (BV), the endothelial cells with a nucleus (N), have prominent nucleolus (Nu) forming the blood-brain barrier. **d, e**) Small ciliated cuboidal ependymal cells lining the brain's ventricles are responsible for the production of cerebrospinal fluid (CSF) (redhead arrow). Note the barrier between CSF and brain tissue (blue arrow). **f**) Small microglia cells (the brain's resident immune cells) with a darkly staining nucleus (N) have heterochromatin (HC) and processes (P) extending toward areas of injury or inflammation. Note the presence of macrophages that can phagocytose pathogens or dead neurons (Ma), lysosomes (Ly), and vacuolated cytoplasm (V).

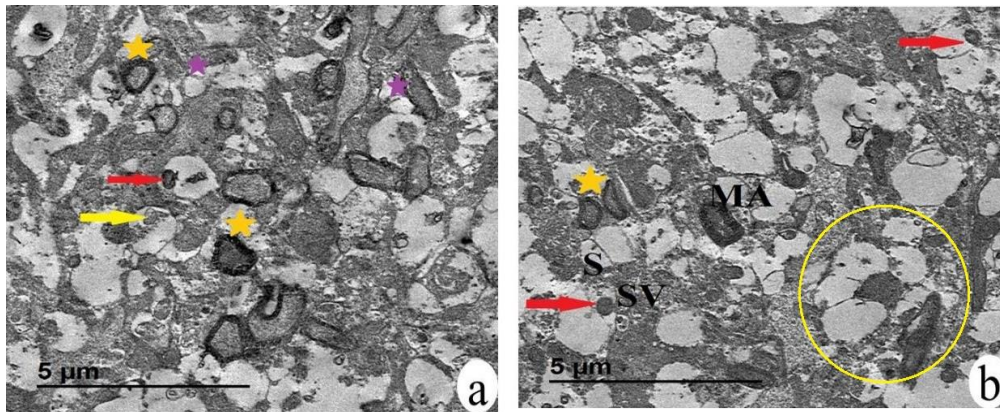


Fig. (6): Transmission electron micrographs of the midline structures (brain stem; medulla oblongata and pons) of *R. hardwickii* showing **a)** Medulla oblongata with myelinated axons (orange star), non-myelinated axons (violet star), with dense neurotransmitter (red arrow) and light clear neurotransmitter (yellow arrow). **b)** Pons containing small oligodendrocytes appeared with a "fried egg appearance" (yellow circle); had myelinated axons (MA, orange star) have a layered appearance due to the myelin sheath and synapse (S) with dense neurotransmitter (red arrow) in synaptic vessel (SV).

Discussion

Bats possess highly specialized and diversified brains across species, attracting significant interest in neuroanatomical research. The application of EM offers distinctive insights into the intricate architecture of the bat brain, aiding in the clarification of its sensory, motor, and cognitive capabilities (Cooper et al., 2024). This study examines the ultrastructure of the normal brain of an adult *R. hardwickii* bat, concentrating on critical regions such as the cerebral cortex, midbrain (hippocampus), cerebellum, medulla oblongata, and pons.

The cerebral cortex of *R. hardwickii* is organized into layers with specific cellular arrangement; the outer layers predominantly consist of axonal layers, abundant in synaptic terminals, whereas the inner ones include pyramidal neurons. The cortical organization and somatosensory cortex display a high density of dendritic spines, believed to be integral to processing sensory signals, synaptic plasticity, spatial navigation, prey detection, and tactile information crucial for flight and roosting behavior.

This finding aligns with studies on *M. brandtii* and *P. pipistrellus* species, wherein the specialized cortex plays a significant role in motor control and cognitive functions that depend heavily on echolocation (Kowalski et al., 1996). It also shows high synaptic specialization and complexity associated with high-frequency sound waves and echoic signals; this is similar to the bats that rely heavily on echolocation, such as those in the family Vespertilionidae, which exhibit particularly dense and specialized synaptic networks in these regions (Feng & Popper, 1998; Schreiner & Winer, 2007; Yartsev et al., 2011; Shu et al., 2015).

The hippocampus of *R. hardwickii* possesses a well-developed granule cell layer similar to that of other mammals (Yartsev et al., 2011; Shu et al., 2015). It is integral to spatial memory and navigation, vital for bats' capacity to recall roosting locations and feeding paths. This result demonstrates significant synaptic plasticity, characterized by frequent alterations of dendritic spines, underscoring the role of experience and environmental

interaction in forming of memory networks. This plasticity facilitates the retention of intricate flight trajectories and navigation through obstructed environments, particularly when echolocation feedback offers abundant sensory information for updating spatial representations, aligning with findings reported by **Suthers et al., (2015)**.

This study demonstrates a highly organized arrangement of Purkinje cells and granule cells in the cerebellum both of which are essential for regulating of movement and balance during flight. The synaptic inputs to Purkinje cells are abundant, and their axonal outputs facilitate the regulation of fine motor skills essential for flight control. This demonstrates significant adaptation for muscle movement control which is crucial for the high maneuverability required in bat flight and echolocation. This finding parallels with that of *Pipistrellus savii* and *Rhinolophus ferrumequinum*, where the cerebellum is highly specialized for maintaining stability and control during aerial maneuvers associated with echolocation, such as hovering and sharp turns (**Shu et al., 2015; Huang & Xu, 2017**).

Conclusion

The *R. hardwickii* brain exhibits a highly organized and specialized structure, characteristic of its evolutionary adaptations for flight, echolocation, and nocturnal lifestyles. Electron microscopy has revealed that the neuronal organization in this bat brain is mainly similar to that of other mammals but with certain distinct features; the neurons are typically large, with a prominent nucleus and well-developed synaptic vesicles. Notably, the synaptic architecture is highly dynamic, with many dense and light neurotransmitters

reflecting the functional demands of complex behaviors. In conclusion, there is variation in the brain structure of insectivorous bat *R. hardwickii* that use echolocation extensively and show heightened auditory processing areas in contrast to nectar-feeding bats, which rely heavily on their sense of vision, tend to have a more developed visual cortex. These differences highlight the adaptability of the *R. hardwickii* brain and its specialization to the ecological niches. Also, the morphology of the bat brain reflects differences in the structural organization of synaptic junctions, the density of dendritic spines, and the configuration of neuronal networks. These variations provide insight into the functional adaptations of *R. hardwickii*, whether for hunting, navigation, or social interactions.

Declarations

Ethics approval and consent to participate

All studies complied with the guidelines established by the Animal Ethical Committee of the Faculty of Science, Tanta University, Egypt.

Consent for publication

The authors affirm their consent to publish this work.

Availability of data and materials

By our institute's regulations, the datasets produced and examined in this study are publicly accessible.

Competing interests

The authors assert that they possess no conflicting interests.

Funding

This research did not obtain specific financing from public, commercial, or non-profit entities.

Authors' contributions

Eman E. El-Nahass: Conceptualization; data curation; formal analysis;

methodology; management; resources; software; validation; original draft writing; review and editing. **Atteyat A. Selim:** Formal analysis; methodology; resources; software; visualization; original draft composition; review and editing. **Omnia M. Shahin:** Formal analysis; inquiry; software development; writing-review and editing.

Acknowledgment

The authors thank the hunters for obtaining bats to complete this study.

References

- Anderson, J.C.; Douglas, R.J.; Martin, K.A.; Nelson, J.C. (1994).** Map of the synapses formed with the dendrites of spiny stellate neurons of cat visual cortex. *J. Comp. Neurol.*, 341(1): 25–38.
<https://doi.org/10.1002/cne.903410104>.
- Baumel, J.J.; King, A.S.; Breazile, J.E.; Evans, H.E.; Vanden Berge, J.C. (1993).** Nomina Anatomica Avium. Handbook of Avian Anatomy. 2nd ed., Ch. 4. Nuttall Ornithological Club, Cambridge, Massachusetts, 45- 132.
- Bozzola, J.J.; Russell, L.D. (1992).** The past, present, and future of electron microscopy. In: Bozzola JJ, Russell LD, editors. Electron microscopy. 1st ed. Boston: Jones and Bartlett Publishers, Inc.; p. 2-14.
- Bourne, J.N.; Harris, K.M. (2012).** Nanoscale analysis of structural synaptic plasticity. *Curr. Opin. Neurol.*, 22(3): 372–382.
<https://doi.org/10.1016/j.conb.2011.10.019>.
- Chung, W.S.; Allen, N.J.; Eroglu, C. (2015).** Astrocytes control synapse formation, function, and elimination. Cold Spring Harb. *Perspect. Biol.* 7(9):a020370. doi: 10.1101/cshperspect.a020370.
- Cooper, L.N.; Ansari, M.Y.; Capshaw, G.; Galazyuk, A.; Lauer, A.M.; Moss, C.F.; Sears, K.E.; Stewart, M.; Teeling, E.C.; Wilkinson, G.S.; Wilson, R.C.; Zwaka, T.P.; Orman, R. (2024).** Bats as instructive animal models for studying longevity and aging. *Ann. NY Acad. Sci.*, 1541(1): 10–23. doi:10.1111/nyas.15233.
- DeFelipe, J. (2010).** From the connectome to the synaptome: an epic love story. *Science* (New York, N.Y.), 330(6008), 1198–1201. doi: 10.1126/science.1193378.
- Feng, A. S., & Popper, A. N. (1998).** Bat Bioacoustics. Springer.
- Gray, E. (1959).** Electron Microscopy of Synaptic Contacts on Dendrite Spines of the Cerebral Cortex. *Nature* 183: 1592–1593.
<https://doi.org/10.1038/1831592a0>.
- Huang, L., & Xu, L. (2017).** "Ultrastructure and functional analysis of the cerebellum in bats." *Journal of Neurobiology*, 75(5): 1-12.
- Kandyel, R.M.; Elwan, M.M.; Abumandour, M.M.A; El Nahass, E.E. (2021).** Comparative ultrastructural-functional characterizations of the skin in three reptile species; *Chalcides ocellatus*, *Uromastyx aegyptia aegyptia*, and *Psammophis schokari aegyptia* (FORSKAL, 1775): Adaptive strategies to their habitat. *Microsc. Res. Tech.*; 84(9): 2104-2118. doi:10.1002/jemt.23766.
- Kang, H.S.; Oh, Y.K.; Cho, B.P.; Lee, Y.D. (1985).** An Electron Microscopic Study on the Hypothalamus of the Hibernating Bat I. Fine Structure of the Nerve Cell. *Applied Microscopy*, 15(2): 10-18.

- Kettenmann, H.; Kirchhoff, F.; Verkhratsky, A. (2013).** Microglia: new roles for the synaptic stripper. *Neuron*, 77(1): 10–18. <https://doi.org/10.1016/j.neuron.2012.12.023>.
- Knott, G.; Genoud, C. (2013).** Is EM dead? *J. Cell Sci.*, 126 (Pt 20): 4545–4552. [10.1242/jcs.124123](https://doi.org/10.1242/jcs.124123).
- Knott, G.; Marchman, H.; Wall, D.; Lich, B. (2008).** Serial section scanning electron microscopy of adult brain tissue using focused ion beam milling. *J Neurosci.: the official journal of the Society for Neuroscience*, 28(12): 2959–2964. <https://doi.org/10.1523/JNEUROSCI.3189-07.2008>.
- Kowalski, J., Nothwang, H. G., & Schreiner, C. E. (1996).** "Tonotopic organization and frequency representation in the bat auditory cortex." *Journal of Neuroscience*, 16(5): 1455-1469.
- Li, A.; Gong, H.; Zhang, B.; Wang, Q.; Yan, C.; Wu, J.; Liu, Q.; Zeng, S.; Luo, Q. (2010).** Micro-optical sectioning tomography to obtain a high-resolution atlas of the mouse brain. *Science (New York, N.Y.)*, 330(6009): 1404-1408. <https://doi.org/10.1126/science.1191776>.
- Nahirney, P.C.; Reeson, P.; Brown, C.E. (2016).** Ultrastructural analysis of blood-brain barrier breakdown in the peri-infarct zone in young adult and aged mice. *J. Cereb. Blood Flow Metab.* 36(2): 413–425. [10.1177/0271678X15608396](https://doi.org/10.1177/0271678X15608396).
- Paolicelli, R.C.; Bolasco, G.; Pagani, F.; Maggi, L.; Scianni, M.; Panzanelli, P.; Giustetto, M., Ferreira, T.A.; Guiducci, E.; Dumas, L.; Ragozzino, D. ; Gross, C.T. (2011).** Synaptic pruning by microglia is necessary for normal brain development. *Science (New York, N.Y.)*, 333(6048): 1456–1458. <https://doi.org/10.1126/science.1202529>.
- Savage, J.C.; Picard, K.; González-Ibáñez, F.; Tremblay, MÈ. (2018).** A Brief History of Microglial Ultrastructure: Distinctive Features, Phenotypes, and Functions Discovered Over the Past 60 Years by Electron Microscopy. *Front. Immunol.*, 9: 803. <https://doi.org/10.3389/fimmu.2018.00803>.
- Schafer, D.P.; Lehrman, E.K.; Kautzman, A.G.; Koyama, R.; Mardinly, A.R.; Yamasaki, R.; Ransohoff, R.M.; Greenberg, M.E.; Barres, B.A.; Stevens, B. (2012).** Microglia sculpt postnatal neural circuits in an activity and complement-dependent manner. *Neuron*, 74(4): 691–705. <https://doi.org/10.1016/j.neuron.2012.03.026>.
- Schreiner, C.E., & Winer, J.A. (2007).** "Auditory cortical field homologies: Implications for understanding the evolution of sound processing." *Hearing Research*, 229(1-2): 52-63.
- Shu, Y.; Liu, Y.; Wang, H. (2015).** "Synaptic organization in the hippocampus of echolocating bats." *Neuroscience Letters*, 595: 1-6.
- Spurr, A.R. (1969).** A low-viscosity epoxy resin embedding medium for electron microscopy. *J. Ultrastruct. Res.*, 26(1): 31-43. [https://doi:10.1016/s0022-5320\(69\)90033-1](https://doi.org/10.1016/s0022-5320(69)90033-1).
- Suthers, R. A., & Hartley, R. A. (2015).** "Motor control and echolocation in bats." *Philosophical Transactions of the Royal Society B: Biological Sciences*, 370(1665), 20140095.

- Theodosius, D.T.; Poulain, D.A.; Oliet, S.H. (2008).** Activity-dependent structural and functional plasticity of astrocyte-neuron interactions. *Physiological reviews*, 88(3): 983–1008. <https://doi.org/10.1152/physrev.00036>. 2007.
- Tremblay, M.È.; Lowery, R.L.; Majewska, A.K. (2010).** Microglial interactions with synapses are modulated by visual experience. *PLoS biology*, 8(11): e1000527. <https://doi.org/10.1371/journal.pbio.100527>.
- Turégano-López, M.; Pozas, F.; Santuy, A.; Rodríguez, J.; Defelipe, J.; Merchan-Perez, A. (2024).** Tracing nerve fibers with volume electron microscopy to quantitatively analyze brain connectivity. *Communications Biology*. 7: 796. <https://doi.org/10.1038/s42003-024-06491-0>
- Verkhratsky, A.; Nedergaard, M. (2018).** Physiology of Astroglia. *Physiol. Rev.*, 98(1): 239–389. <https://doi.org/10.1152/physrev.00042>. 2016
- White, E.L.; Rock, M.P. (1980).** Three-dimensional aspects and synaptic relationships of a Golgi-impregnated spiny stellate cell reconstructed from serial thin sections. *J. Neurocytol*, 9(5): 615–636. <https://doi.org/10.1007/BF01205029>.
- Yartsev, M. M., & Witter, M. P. (2011).** "Mapping the spatial memory network in the bat brain." *Nature Neuroscience*, 14(6): 781-789.

دراسة التركيب الدقيق للتشريح العصبي للمخ في خفاش *Rhinopoma hardwickii* البالغ

د. ايمان النحاس، ا.د. عطيات سليم، أمينة شاهين

قسم علم الحيوان- كلية العلوم- جامعة طنطا

ينتمي خفاش *R. hardwickii* الي فصيلة Microchiroptera التي تتميز بتحديد الموقع بالصدى أثناء الطيران، على عكس الخفافيش من فصيلة Megachiroptera. تهدف هذه الدراسة إلى فحص التركيب الدقيق لمختلف مناطق المخ في الخفاش البالغ *R. hardwickii*. تم تخدير الخفافيش ثم اجراء القتل الرحيم عن طريق خلع الدماغ. يتم التشريح وحفظ عينات المخ في الجلتزر الدهيد، ثم غسلها بمحلول cacodylate، ثم تثبت بمحلول osmium tetroxide. بعد ذلك يتم ازالة الماء الزائد من العينات باستخدام الكحول الإيثيلي، ثم تغمر في epoxy resin. لفحص الأنسجة يتم صبغة الشرائح بأزرق التولويدين. يتم تقطيع شرائح ultra sections وصبغتها بثنائي هيدرات أسيتات اليورانيل ومحلول سترات الرصاص المشبع. فُحصت الشرائح وصُوّرت باستخدام الميكروسكوب الالكتروني النافذ. من خلال النتائج وجد ان المخ ينقسم إلى ثلاث مناطق: المخ الأمامي، والمخ المتوسط، والمخ الخلفي. باستخدام الميكروسكوب الإلكتروني النافذ وجد ان المخ يتكون من أوعية دموية ونوعين من الخلايا: الخلايا العصبية والخلايا الداعمة لها. ظهرت الخلايا العصبية كخلايا كبيرة ذات نوى كبيرة، وكثافة كروماتينية منتشرة، ونوية بارزة، ونهايات عصبية. تلك الخلايا لها نوعان: ١. خلايا هرمية كبيرة على شكل قنينة ذات شجرة دندريته قمية واحدة قوية ومحاذية للقشرة وعدة شجرات دندريته قاعدية. ٢. خلايا صغيرة غير هرمية قد تكون نجمية أو خلايا حبيبية. الخلايا الداعمة ظهرت متطورة جيداً، خاصة في المخيخ، ولها أربعة أنواع: الخلايا النجمية، الخلايا الدبقية الصغيرة، الخلايا الدبقية قليلة التغصن، والخلايا البطانية. من خلال النتائج وجد ان مخ *R. hardwickii* يتميز بحجمه الصغير وزيادة عدد الخلايا العصبية المتطورة بشكل جيد، خاصة في المخيخ، مقارنة بأجزاء الدماغ الأخرى؛ من الدراسة يتبين ان مخ خفاش *R. hardwickii* يتميز بسمات عصبية مرتبطة بالصدى الصوتي، مما يكشف عن التوافقات والعلاقات التطورية للخفافيش مع بعضها.